Research on Engineering Structures & Materials
www.jresm.org
Research Group

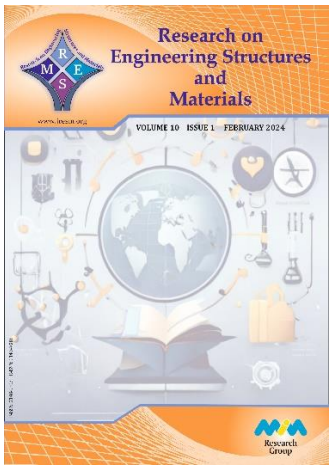


# Experimental study on the effect of colloidal nano silica in self-compacting concrete containing ground granulated blast furnace slag

K. Shyam Sundar Murty, G.V. Rama Rao, S. Adiseshu

Online Publication Date: 30 March 2023
URL: http://www.jresm.org/archive/resm2024.105me1204rs.html
DOI: http://dx.doi.org/10.17515/resm2024.105me1204rs

Journal Abbreviation: *Res. Eng. Struct. Mater.*

**To cite this article**
Murty KSS, G.V. Rao R, Adiseshu S. Experimental study on the effect of colloidal nano silica in self-compacting concrete containing ground granulated blast furnace slag. *Res. Eng. Struct. Mater.*, 2024; 10(4): 1467-1481.

Research on Engineering Structures & Materials
www.jresm.org
Research Group

*Research Article*

# Experimental study on the effect of colloidal nano silica in self-compacting concrete containing ground granulated blast furnace slag

K. Shyam Sundar Murty*[,a], G.V. Rama Rao[b], S. Adiseshu[c]

*Department of Civil Engineering, Andhra University, Visakhapatnam, India*

**Article Info**

*Article history:*

Received 02 Dec 2023
Accepted 23 Mar 2024

*Keywords:*

*Colloidal nano silica;*
*Self-compacting concrete;*
*Flowability*

**Abstract**

Self-compacting concrete (SCC) is profusely utilized in building construction due to its unique design and mechanism of flow without segregation by occupying the corners and preventing the voids to achieve better compaction and mechanical strength. This work addresses the effect of colloidal nano-silica (NS) of size 5-40nm with an active nano solids content of 32% on SCC containing Ground Granulated Blast Furnace Slag (GGBFS) and Ordinary Portland Cement as binders in addition to NS. The liquid content of 68% in NS was added to the water content in the mix. The ratios of NS were evaluated at 0%,0.5%,1%,1.5%, 2% and GGBFS as 20% by weight of binder in concrete. The water to binder ratio was 0.33 with a water and binder content of 184kg/m$^3$ and 557.58 kg/m$^3$. The optimum mix was 1.5% NS based on the concrete's slump and compressive strength at 28 days. The slump was reduced with a rise in NS beyond 1.5% due to the accumulation of NS particles causing the reduction in flowability. The density of SCC for all the mixes was satisfactory. The compressive strength of optimum SCC, $M_2$1.5NS20G was decreased by 5.88% and increased by 0.49% and 2.45% at 7, 28 and 91 days to that of the reference mix whereas its split tensile strength was risen by 31.13%, 9.27%, and 12.41% and flexural strength was risen by 5.8% and reduced by 8.17% and 4.06% to that of the reference mix at aforementioned durations. The SEM and XRD analyses were conducted on the optimum hardened SCC mix at 28 days in which the presence of Calcium silicate hydrate compounds of different crystalline structures, viz., Ettringite, and Portlandite were observed. The SCC designed in the work can be used for structural applications such as beam-column joints.



## 1. Introduction

Self-compacting concrete (SCC) is extensively utilized in the construction sector and was first proposed in 1986 with the development of the first prototype in 1988 in Japan using the materials available in the market, to solve labour scarcity, achieve durable structures with good compaction without vibration, thereby reducing the voids in members and at the junctions of congested reinforcements [1-4]. The method uses a superplasticizer, meagre aggregate content, and a lower ratio of water and powder to attain self-compaction, high deformability, viscosity, and hindrance to segregation during the concrete flow through the congested reinforcement [1-2]. As the gap between the particles diminishes, the number of collisions per unit of time, interparticle contact and internal stress rise as the concrete deforms, especially near obstructions [1]. The thickening of shear in SCC, which is caused by the cluster formations of Brownian motion of small particles that lead the viscosity to increase the shear rate, is significant to be considered to prevent the damage of mixers, conduits, and pipes [7]. The packing density of total

*Corresponding author: kssundar.phd@andhrauniversity.edu.in
[a] orcid.org/0000-0001-5138-9448; [b] orcid.org/0000-0002-3443-8890; [c] orcid.org/0000-0001-9415-0453
DOI: http://dx.doi.org/10.17515/resm2024.105me1204rs

aggregate in SCC lies between 50% and 60% to decrease the relation between them and limit the shear deformation of concrete [1-2]. The pressure transferability occurs when mortar undergoes normal stress between coarse aggregate particles [1,5]. The reduction in shear deformation of mortar relies on the solid particles' behaviour in the mortar [6]. Industrial waste such as GGBFS, fly ash, etc. containing pozzolanic behaviour are used in SCC, to avoid their disposal onto the land [9]. The enhancement of the strengths of SCC depends on the proportion of SCM to be replaced or added to the cement [9-13]. There were no standard guidelines for the Self-Compacting concrete mix design during its entry into the construction market and the construction companies had proposed their procedures for the concrete [14]. In the year 2005, guidelines were proposed for SCC, receiving international recognition [15]. India had also adopted the guidelines for SCC in IS 10262:2019 Concrete Mix Design Proportions [16].

GGBFS, a final byproduct obtained from steel making, contains calcium oxide and silica in major proportions, and alumina and Magnesia in minor proportions. 'The hydraulic capability of GGBFS was first discovered by Emil Langen in Germany in 1862' and its commercial production was commenced in 1865 [17]. Later, it was widely spread across Europe to produce Portland slag cement to be used in underground structures to oppose the aggressive conditions in the ground [17]. The grinding of GGBFS was carried out by two processes viz. wet process [18], with limitations having developed by Victor Trief in Belgium, and dry process that was further adopted successfully [17]. The hydraulic activity of GGBFS depends on the chemical composition that determines its basicity index with the quick lime-to-silica ratio to be greater than 1[19] and it is enhanced with increasing calcium, magnesium, and aluminum oxide ranges and diminished with rising silica in water [20]. GGBFS causes variations in hydration products due to C-S-H gel, resulting in larger pore volumes in the cement matrix, high water absorption, and reduced strength. The activated alumina further reacts with portlandite and gypsum to produce Ettringite [21,22]. GGBFS has a superior water reduction effect and reduces the time-dependent loss of slump flow and fluidity [23]. Workability is reduced by the huge surface area with uneven surface texture of GGBFS [24]. Superplasticizer (SP) improves the performance of fresh mixture and disperses the powder particles through steric repulsion and its adsorption on cement particles might lower the initial hydration resulting in slow setting as well as initial strength growth of the paste [25]. GGBFS occupies the spaces in the aggregate to form denser concrete and influences the development of strength in SCC which depends on water-to-cement (w/c) ratio and quantity of GGBFS with the former's increase leading to the increase in the latter at the three different percentages of slag [26]. Compression, split tension and flexure of concrete are increased up to 20% substitution of GGBFS beyond which they are reduced due to a dearth of flowability [24, 26, 27] and dilution effect that forms the alkali–silica reaction with a huge amount of unreactive silica present in GGBFS [28]. The alkali-silica reaction stresses the concrete to enlarge forming the cracks [29].

Colloidal nano silica (NS), obtained from the Weber Stober process [30], contains dense, 'amorphous hydroxylated silica particles' of size 1-100 nm in an aqueous form [31], is used in the construction sector [32,33]. The vast specific surface area of NS contributes to an aggregate-cement binder [34] and entails a high water–cement ratio. A higher quantity of PCE-based super-plasticizer is used to enhance flow properties to reduce particle agglomeration, and improper dispersion, and improve workability [35,43]. PCE improves NS dispersion and compressive strength of mortar and lowers the porosity and dangerous voids in hardened cement paste [36]. Well–dispersed nanoparticles activate to improve the hydration and consume the portlandite to form excess C-S-H gel during pozzolanic reactions [37-39] and thicken the cement paste [39]. The concrete's initial age strength is increased and its initial and final setting times are shortened by nano silica particles [40].

The ITZ is also improved by the packing of smaller particles in all voids to decrease permeability [41]. When the amount of NS increases, the slump reduces due to the formation of silanol groups and inadequate water [42]. Adding up to 2% to 3% of NS as a replacement for cement in concrete can enhance its strength by leveraging its pozzolanic reactivity and filling action [43-45].

Considering the previous research works on colloidal nano silica, it has been noted that the separate addition of NS solids content to binder materials and NS liquid content to the water and their effect on the workability and mechanical strengths of SCC were not discussed. The objective of the current research work is to investigate workability properties, mechanical strength properties and microstructural analysis of the high-strength self-compacting concrete of Grade 50 incorporated with cement, GGBFS and colloidal nano silica (32% solids and 68% liquid) as cementitious materials and Auramix 300 plus as superplasticizer of PCE type.

## 2. Experimental Work

### 2.1 Materials

Ordinary Portland Cement 53 grade of KCP brand, confirming to IS 269:2015 [49] and GGBFS, confirming to IS 16714-2018 [50], the by-product of Visakhapatnam Steel Plant, were used in concrete mix and their chemical and physical characteristics are presented in Table 1 and Table 2 respectively. Colloidal Nano silica, designated as CemSyn XTX*, having a specific gravity of 1.22, was manufactured and procured from Beechems, Kanpur, Uttar Pradesh, India. The solid particles visible in Transmission Electron Microscopy image as shown in Fig. 1, contain active nano silica with liquid among them.

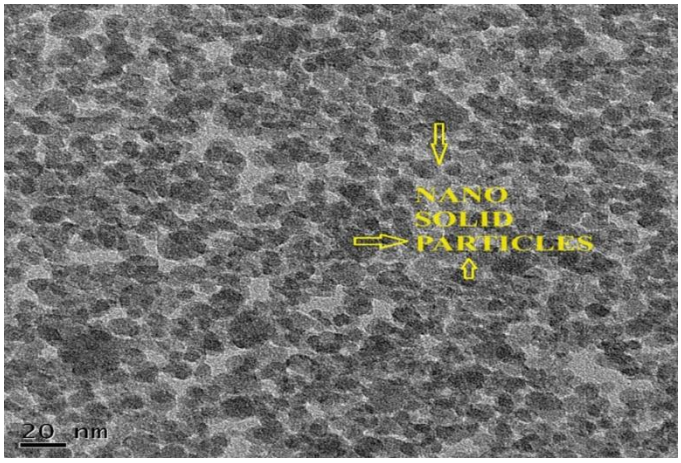


Fig. 1. TEM image of Colloidal Nano Silica

Coarse aggregate of size 10mm, having specific gravity 2.88, confirming to IS 383:2016 [51], was obtained from Anjani Stone Crushers, Duddupalem, Anakapalli, India. River sand of type Zone – II having Fineness modulus 2.66 and specific gravity 2.61, confirming to IS 383:2016, was utilized as fine aggregate in concrete mix [51]. Chemical admixture, Auramix 300 Plus of specific gravity 1.08**, which contains Viscosity Modifying Admixture procured from FOSROC, confirming to IS 9103-1999 [52], was used in SCC. Potable water was used during the concrete mixing.

Table 1. Chemical characteristics

| Sl. No. | Characteristic | OPC 53*** | Requirements as per IS 269:2015 | GGBFS**** | Requirements as per IS 16714:2018 |
|---|---|---|---|---|---|
| 1 | Lime Saturation Factor | 0.92 | 0.8-1.02 | - | - |
| 2 | Ratio of percentage of Alumina to that of Iron Oxide | 1.24 | Min. 0.66 | - | - |
| 3 | Insoluble Residue (% by mass) | 0.47 | Max. 5.0 | 0.78 | Max. 3.0 |
| 4 | Magnesia (% by mass) | 1.10 | Max. 6.0 | 8.86 | Max. 17 |
| 5 | Sulphuric Anhydride (% by mass) | 1.74 | Max. 3.5 | 0.66 | Max. 3 |
| 6 | Total loss of ignition (%) | 1.24 | Max. 4.0 | NIL | Max. 3 |
| 7 | Chlorides (%) | 0.002 | Max. 0.1 | 0.012 | Max. 0.1 |
| 8 | Manganese Oxide (%) | - | - | 0.72 | Max. 5.5 |
| 9 | Sulphide Sulphur (%) | - | - | 0.78 | Max. 2 |

Table 2. Physical characteristics

| Sl. No. | Characteristic | OPC 53 | Requirements as per IS 269:2015 | GGBFS | Requirements as per BS 6699:1992 |
|---|---|---|---|---|---|
| 1 | Fineness ($m^2/kg$) | 299*** | Min. 225 | 342**** | Min. 275 |
| 2 | Soundness LeChatelier Expansion(mm) | 0.5 | Max. 10 | NIL | Max. 10 |
| 3 | Initial Setting Time (min.) | 165 | Min. 30 | 185 | More than 30 |
| 4 | Normal Consistency (%) | 29.5 | - | 29 | - |
| 5 | Specific gravity | 3.13 | - | 2.9 | - |
| 6 | Compressive strength (MPa) 7 days | 49 | Min. 37 | 29 | Min. 12.0 |
| | 28 days | 60 | Min. 53 | 49 | Min. 32.5 |

Courtesy: *Bee Chems, Kanpur, Uttar Pradesh, India

**FOSROC constructive solutions

***KCP Cement Limited, Andhra Pradesh, India

**** Sri Vishnu Sai Saravana Enterprises, Autonagar, Visakhapatnam, India

### 2.2 SCC Mix Design

In this research work, with reference to IS 10262:2019 [16], the standard deviation of concrete of Grade is 5N/mm$^2$. The mean target strength of the concrete of grade 50 is 58.25 N/mm$^2$. The entrapped air content was taken as 1.5% of the volume of concrete for the nominal aggregate maximum size of 10mm. GGBFS was taken at a proportion of 20% [24,26,27] and the solids content in colloidal nano silica was taken in different proportions of 0%, 0.5%, 1%,1.5% and 2% by weight of the binder content and liquid content was added to the potable water by calculating it separately. The remaining proportion of the binder material contains cement. Based on the trials, the water to binder ratio was adopted to be 0.33 with the binder material and water content as 557.57 kg/m$^3$ and 184 kg/m$^3$. The influence of GGBFS on the fresh SCC depends on the fineness and admixture proportion as it retains water at increased fineness to lower fluidity and slump flow [24,26,27]. The admixture was considered 0.5% for concrete containing 0% NS and 0.7% for concrete containing the rest of the proportions of NS by weight of binder content. The mixes were given notation as mentioned in Table 3. The fines required were then calculated. The percentage of particles passing through 0.125 mm IS sieve was 3%. The total aggregate quantity was obtained in which fine aggregate lies within the limits of 48% to 60%. Water to-powder ratio was within the limits.

Table 3. Quantity of constituents in SCC

| Mix Notation / Constituents | $M_2$0NS 20G | $M_2$0.5NS 20G | $M_2$1NS 20G | $M_2$1.5NS 20G | $M_2$2NS 20G |
|---|---|---|---|---|---|
| Cement (kg/m$^3$) | 446.06 | 445.17 | 444.28 | 443.38 | 442.49 |
| GGBFS (kg/m$^3$) | 111.52 | 111.52 | 111.52 | 111.52 | 111.52 |
| NS (kg/m$^3$) | 0 | 2.79 | 5.58 | 8.36 | 11.15 |
| NS(Solids) (kg/m$^3$) | 0 | 0.89 | 1.78 | 2.68 | 3.57 |
| NS(Liquids) (kg/m$^3$) | 0 | 1.89 | 3.79 | 5.69 | 7.58 |
| Water (kg/m$^3$) | 184 | 184 | 184 | 184 | 184 |
| Fine Aggregate (kg/m$^3$) | 814.14 | 814.14 | 814.14 | 814.14 | 814.14 |
| Coarse Aggregate (kg/m$^3$) | 879.9 | 871.17 | 865.41 | 859.65 | 853.89 |
| Chemical Admixture (kg/m$^3$) | 2.79 | 3.90 | 3.90 | 3.90 | 3.9 |
| water-binder ratio | 0.33 | 0.33 | 0.33 | 0.33 | 0.33 |
| Fines required (kg/m$^3$) | 24.42 | 24.42 | 24.42 | 24.42 | 24.42 |
| Powder content (kg/m$^3$) | 582 | 582 | 582 | 582 | 582 |
| Water powder ratio by volume | 0.97 | 0.96 | 0.96 | 0.96 | 0.96 |

$M_2$ 0NS 20G  $M_2$ = M 50  0NS = 0% NS  20G = 20% GGBFS

The constituents were mixed in the concrete mixer. The fresh concrete was tested for its workability after mixing as shown in Fig.2. The flow table was allowed to rotate and subjected to impact as shown in Fig.2(a). The concrete was spread horizontally throughout the circumference of the table considering a maximum distance(mm) between the far ends to be slump indicating the flowability as shown in Fig.2(b). The concrete was poured into the V-Funnel to find the viscosity by counting down the time taken (s) to pass through it as shown in Fig.2(c) and in the L-Box through the vertical duct to pass down and move in the horizontal portion to study the passing ability as shown in Fig.2(d) [16].

### 2.3 Preparation of Test Specimens

A total of 45 standard cube specimens of size 150mm x150mmx150mm were cast with the fresh concrete of the five different mixes. They were placed in ambient curing for 24 hours at 27±2°C and then in water curing after demoulding for the different durations of 7, 28, and 91 days [53]. Three specimens of all five mixes were tested for the compressive strength for the corresponding durations. The same procedure was repeated for 45 standard cylindrical specimens of size 150mm diameter and 300 mm length to test for Split Tensile strength and 45 standard prism specimens of size 100mm x 100mm x500mm to test for flexural strength [53]. The notations for the specimens were considered as $M_2$0NS20G (reference mix), $M_2$0.5NS20G, $M_2$1NS20G, $M_2$1.5NS20G and $M_2$2NS20G.

## 3. Results and Discussions

### 3.1 Workability Tests on SCC

The workability test values of SCC are mentioned in Table 4. The slump of $M_2$ 0NS20G is classified as SF1 and $M_2$0.5NS20G, $M_2$1NS20G and $M_2$1.5NS20G are classified as SF2 [16]. The slump flow of $M_2$2NS20G was very less due to the assemblage of NS particles in the mix. The mix, $M_2$ 0.5 NS 20G, passed completely through the L-box like a liquid [16]. The viscosity of all the mixes exceeded 25 seconds i.e., V2 [16]

Table 4. Fresh properties of SCC

| Mix Notation | Slump(mm) | $h_1$(mm) | $h_2$(mm) | Passing Ability ($h_1$/ $h_2$) | Viscosity(s) |
|---|---|---|---|---|---|
| $M_2$ 0NS 20G | 620 | 53 | 315 | 0.17 | 96.00 |
| $M_2$ 0.5 NS 20G | 670 | 65 | 65 | 1.00 | 32.19 |
| $M_2$ 1NS 20G | 670 | 55 | 128 | 0.43 | 28.40 |
| $M_2$ 1.5NS 20G | 680 | 42 | 210 | 0.20 | 64.95 |
| $M_2$ 2NS 20G | 500 | 40 | 270 | 0.15 | 60.12 |

(a)

(b)

(c) (d)

Fig. 2 Workability tests on scc (a) flow table equipment, (b) slump flow, (c) viscosity test, and (d) passing ability test using L-Box

### 3.2 Compressive Strength

The strength of $M_20.5NS20G$, $M_21NS20G$, $M_21.5NS20G$ and $M_22NS20G$ was decreased by 9.25%, 4.20%, 5.88%, and 17.09% to that of the reference mix, $M_20NS20G$ at 7 days and the tests were conducted on 300T compression testing machine as shown in Fig.4. Similarly, the strength of $M_20.5NS20G$, $M_21NS20G$, $M_22NS20G$ was decreased by 7.60%, 6.52%, 4.34% and $M_21.5NS20G$ increased by 0.49% of that of the reference mix at 28 days. The strength of $M_20.5NS20G$, $M_21NS20G$, $M_22NS20G$ was decreased by 5.89%, 3.20%, 11.92% and $M_21.5NS20G$ increased by 2.45% to that of the reference mix at 91 days respectively as shown in Fig.3.

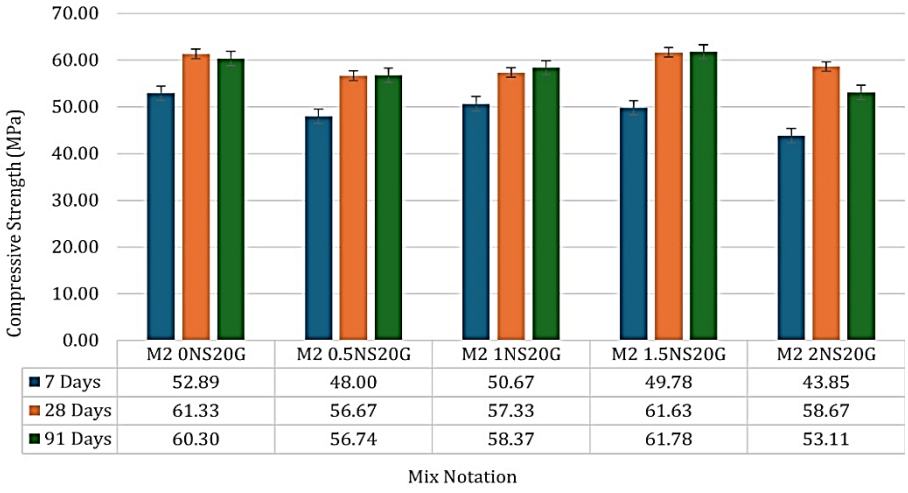


| | M2 0NS20G | M2 0.5NS20G | M2 1NS20G | M2 1.5NS20G | M2 2NS20G |
|---|---|---|---|---|---|
| 7 Days | 52.89 | 48.00 | 50.67 | 49.78 | 43.85 |
| 28 Days | 61.33 | 56.67 | 57.33 | 61.63 | 58.67 |
| 91 Days | 60.30 | 56.74 | 58.37 | 61.78 | 53.11 |

Fig. 3. Variation of compressive strength of SCC at 7,28,91 days

The reduction in strengths of 0.5%,1% NS concrete might be due to the possible lack of dispersion of nanoparticles, which can lead to weak zones [47]. It has been noted that there

is a minor difference in the strength between the reference and optimum mixes except in the slump values and the minute enhancement of compressive strength in the optimum mix was increased by pozzolanic reactivity and the generation of extra C-S-H gel [46]. The mix containing 2% NS in pozzolanic reaction is diminished by its agglomeration and changes the original amorphous C-S-H gel into tobermorite leading to reduced compressive strength [47].


Fig. 4. Compressive strength test using 300T CTM

### 3.3 Split Tensile Strength

The strength of SCC mixes of $M_2$0.5NS20G and $M_2$1NS20G was decreased by 10.38%, 18.87% and $M_2$1.5NS20G, $M_2$2NS20G increased by 31.13% and 20.75% that of the reference mix, $M_2$0NS20G at 7 days and the tests were conducted on 300T compression testing machine as shown in Fig.6.

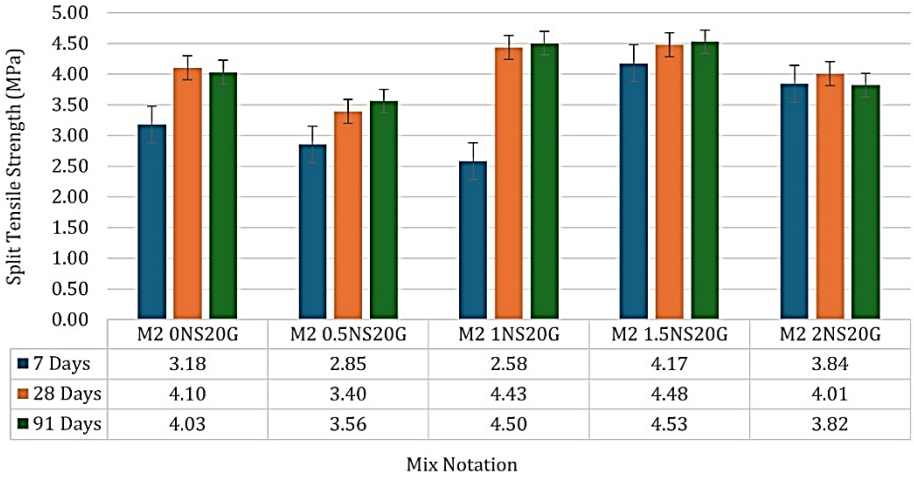


| | M2 0NS20G | M2 0.5NS20G | M2 1NS20G | M2 1.5NS20G | M2 2NS20G |
|---|---|---|---|---|---|
| 7 Days | 3.18 | 2.85 | 2.58 | 4.17 | 3.84 |
| 28 Days | 4.10 | 3.40 | 4.43 | 4.48 | 4.01 |
| 91 Days | 4.03 | 3.56 | 4.50 | 4.53 | 3.82 |

Fig. 5. Variation of split tensile strength of SCC at 7,28,91 days

Similarly, the strength of $M_2$0.5NS20G, $M_2$2NS20G was decreased by 17.07%, 2.19% and M21NS20G and $M_2$1.5NS20G was increased by 8.05%, 9.27% to that of the reference mix

at 28 days. The strength of $M_20.5NS20G$, $M_22NS20G$ was decreased by 11.66%, 5.21% and $M_21NS20G$, $M_21.5NS20G$ increased by 11.66%, 12.41% to that of the reference mix at 91 days respectively as shown in Fig.5. The cause of strength variance when compared to reference mix might be due to the improper nanoparticle dispersion that form weak portions [47]. When the proportion of NS exceeds 1.5%, the excess silica is leached out due to the liberated lime during cement hydration which leads to strength reduction [46,47].


Fig. 6. Split tensile strength test using 300T CTM

### 3.4 Flexural Strength

The strength of SCC mixes of $M_20.5NS20G$, $M_22NS20G$ was decreased by 0.70%, 3.51% and $M_21NS20G$, $M_21.5NS20G$ increased by 5.62%, 5.80% to that of the reference mix, $M_20NS20G$ at 7 days and the tests were carried out on 100T universal testing machine. The strength of $M_20.5NS20G$, $M_21NS20G$, $M_21.5NS20G$ and $M_22NS20G$ was decreased by 13.44%, 8.56%, 8.17% and13.44% to that of the reference mix at 28 days.

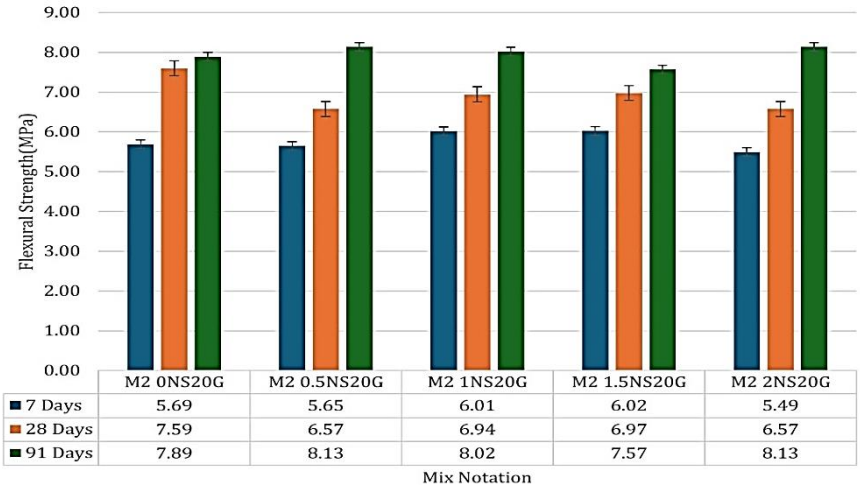


| | M2 0NS20G | M2 0.5NS20G | M2 1NS20G | M2 1.5NS20G | M2 2NS20G |
|---|---|---|---|---|---|
| 7 Days | 5.69 | 5.65 | 6.01 | 6.02 | 5.49 |
| 28 Days | 7.59 | 6.57 | 6.94 | 6.97 | 6.57 |
| 91 Days | 7.89 | 8.13 | 8.02 | 7.57 | 8.13 |

Fig. 7Variation of flexural strength of SCC at 7,28,91 days

The strength of $M_2$1.5NS20G was decreased by 4.06% and $M_2$0.5NS20G, $M_2$1NS20G, $M_2$2NS20G increased by 3.04%, 1.65%, 3.04% that of reference mix at 91 days respectively as shown in Fig.7. Due to the rapid utilization of portlandite produced during the early age hydration of cement due to the high NS reactivity, the flexural strength increased up to 1.5% [48]. However, at 28 days, it decreased in comparison to the reference mix, but it still exceeded the estimated flexural strength as per IS 456:2000 [54] and the required slump was achieved.

Fig. 8. Flexural strength test using 100T UTM

### 3.5 Microstructural studies on SCC

Scanning Electron Microscopy (SEM) and X-ray Diffraction (XRD) tests were conducted on the optimum SCC mix, $M_2$1.5NS20G at 28 days, to study the compounds present in the concrete. The sample from the cube specimen was taken and ground into the powder using the impact testing equipment and then, it was sieved through 75 micron IS Sieve. The fine powder passed through the sieve was collected for the tests. The powder was compressed to a pill and dispersed in volatile solvent and placed on mounting pin for the test. Scanning Electron Microscope (SEM) test is an instrument used to produce a magnified image to study the internal structure of the material by ejecting electrons instead of light from an electron gun with much higher resolution due to the usage of electromagnets to control the degree of magnification to generate X-rays, backscattered and secondary electrons for image detection.

Fig.9 illustrates the needle-shaped crystals of calcium tri sulfoaluminate or Ettringite, large prismatic crystals of calcium hydroxide and fiber-shaped C-S-H which enhanced strength of concrete. Similarly, NS enhanced the C-S-H gel formation and reduced calcium hydroxide to form a dense concrete structure [37-39].

X-Ray Diffraction [55] is a method to find compounds present in the sample by emitting X-rays from a X-ray tube that is placed on a goniometer along with sample, optics and detector. The powdered sample was placed on a glass slide in sample holder. The number of X-rays scattered by the sample is counted at each angle 2θ by the detector and its position is recorded as 2θ. The X-ray intensity is recorded as counts per unit time. The equipment is connected to Panalytical XPert High Score software (ICDD indexed) to identify the compounds as shown in Fig.10. The long-range order with sharp maxima and peak position indicates the crystalline nature. with Etrringite (Hexacalcium aluminate trisulfate hydrate), Xonotlite and Thaumasite (Calcium silicate hydrates), Yeelimite

(Calcium sulfo aluminate) were identified as crystalline compounds with the parameters of the intensity (height of the peak), Full Width of Half Maximum (crystalline size) and detector angle (2θ).

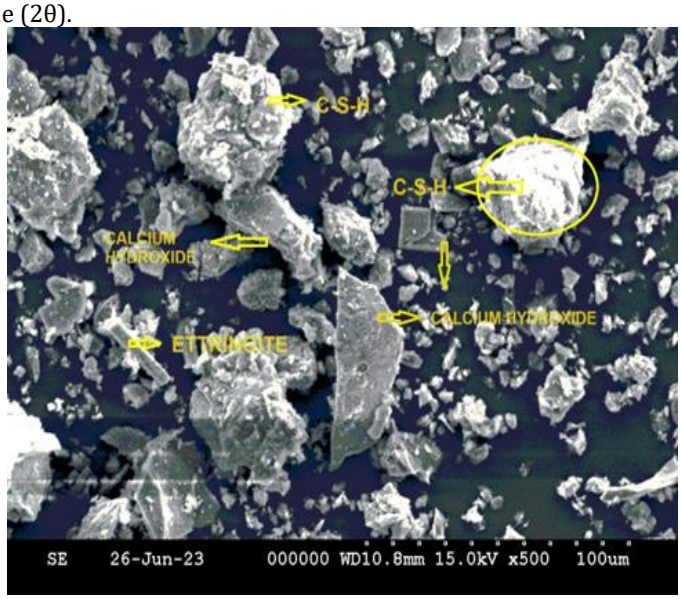


Fig. 9. SEM image of 28 days hardened SCC, $M_2$1.5NS20G

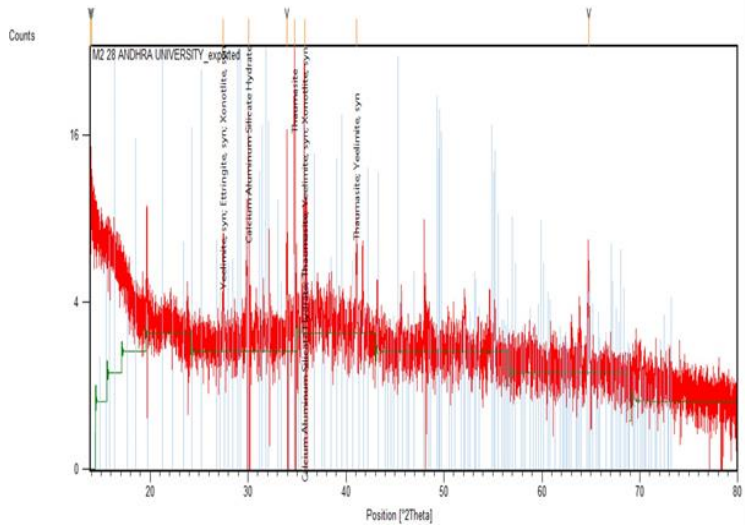


Fig. 10. XRD pattern of 28 days SCC, $M_2$1.5NS20G

## 4. Conclusions

- The slump of the SCC was maximum at 1.5% NS as a binder, beyond which the NS solid particles accumulated and reduced the flow of SCC and the additional amount of superplasticizer (>0.7% of binder material) must be added to maintain the workability of the mix beyond 1.5% NS.

- The compressive strength of optimum SCC was reduced by 5.88% at 7 days and was increased by 0.49% and 2.45% at 28 days and 91 days to that of the reference mix respectively. Despite the minor rise in optimum strength compared to reference mix, the high slump value of the optimum mix was achieved with a significant difference. NS, having a very small particle in size, enhanced the strength due to good pozzolanic activity and filled the voids in SCC, including ITZ, and formed extra C-S-H gel.
- The split tensile strength of optimum SCC at 7, 28 and 91 days was increased by 31.13%, 9.27% and 12.41% to that of the reference mix respectively. When the proportion of NS exceeds 1.5%, the excess silica was leached out due to the liberated lime during cement hydration and strength reduction.
- The flexural strength of optimum SCC was decreased by 8.17% and 4.06% at 28 days and 91 days whereas it was increased by 5.8% at 7 days to that of the reference mix respectively. Its increase of up to 1.5% compared to other NS mixes was due to the quick utilization of portlandite liberated during the cement hydration at early ages due to the high reactivity of NS. Although the flexural strength of the optimum mix is less than that of the reference mix, it exceeded the estimated strength value and achieved the required slump.
- Due to its greater specific surface area, NS functions as a binder between cement and aggregate, shortening the initial and final setting time and improving early age strength.
- SEM and XRD pictures indicated calcium hydroxide and calcium silicate hydrate compounds with different crystalline structures. Strength is primarily due to these compounds. NS also increased C-S-H gel development and lowered calcium hydroxide, resulting in a compact concrete structure.

## 5. Scope for further study

- The current research can be expanded by incorporating a higher concentration of solid particles in the NS and examining its impact on the characteristics of SCC.
- The effect of adding another binder material in SCC in addition to the existing ones, can be investigated.

## References

[1] Okamura H, Ouchi M. Self-Compacting Concrete. Journal of Advanced Concrete Technology 2003;1:5–15. https://doi.org/10.3151/jact.1.5

[2] Hajime Okamura (Prof.) & Kazumasa Ozawa (Assoc. Prof.) Self-Compacting High Performance Concrete, Structural Engineering International, 1996,6:4, 269-270, https://doi.org/10.2749/101686696780496292

[3] Ozawa,K.,Maekawa,K.,Kunishima,M.,and Okamura,H.Development of high-performance concrete based on the durability design of concrete structures.Proceedings of the second East- Asia and Pacific Conference on Structural Engineering and Construction 1989;(EASEC-2), 1, 445-450.

[4] Okamura, H., Maekawa, K., and Ozawa, K.High Performance Concrete.Gihodo Publishing.1993; https://www.researchgate.net/publication/285281222_Development_of_High_Performance_Concrete

[5] Ouchi, M. and Edamatsu, Y. A Simple evaluation method for interaction between coarse aggregate and mortar particles in self-compacting concrete. Transaction of JCI. 2000; https://www.rilem.net/images/publis/pro007-011.pdf

[6] Nagamoto, N., and Ozawa, K.Mixture properties of Self-compacting, High-performance concrete.ACI International, 1997; SP-172, 623-636.

https://www.concrete.org/publications/internationalconcreteabstractsportal/m/details/id/6155
[7] Feys D, Verhoeven R, De Schutter G. Why is fresh self-compacting concrete shear thickening? Cement and Concrete Research 2009;39:510–23. https://doi.org/10.1016/j.cemconres.2009.03.004
[8] Nandhini K, Karthikeyan J. A review on sustainable production of self-compacting concrete utilizing industrial by-products as cementitious materials. Innovative Infrastructure Solutions 2022;7. https://doi.org/10.1007/s41062-022-00792-1
[9] Mahalingam B, Nagamani K, Kannan LS, Mohammed Haneefa K, Bahurudeen A. Assessment of hardened characteristics of raw fly ash blended self-compacting concrete. Perspectives in Science 2016;8:709–11. https://doi.org/10.1016/j.pisc.2016.06.066
[10] Esquinas AR, Ledesma EF, Otero R, Jiménez JR, Fernández JM. Mechanical behaviour of self-compacting concrete made with non-conforming fly ash from coal-fired power plants. Construction and Building Materials 2018;182:385–98. https://doi.org/10.1016/j.conbuildmat.2018.06.094
[11] Altoubat S, Talha Junaid M, Leblouba M, Badran D. Effectiveness of fly ash on the restrained shrinkage cracking resistance of self-compacting concrete. Cement and Concrete Composites 2017;79:9–20. https://doi.org/10.1016/j.cemconcomp.2017.01.010
[12] Benaicha M, Roguiez X, Jalbaud O, Burtschell Y, Alaoui AH. Influence of silica fume and viscosity modifying agent on the mechanical and rheological behavior of self compacting concrete. Construction and Building Materials 2015;84:103–10. https://doi.org/10.1016/j.conbuildmat.2015.03.061
[13] Fakhri M, Yousefian F, Amoosoltani E, Aliha MRM, Berto F. Combined effects of recycled crumb rubber and silica fume on mechanical properties and mode I fracture toughness of self-compacting concrete. Fatigue & Fracture of Engineering Materials & Structures 2021;44:2659–73. https://doi.org/10.1111/ffe.13521
[14] Geert De Schutter, Peter J.M.Bartos, Peter Domone, John Gibbs. Self-Compacting Concrete. Whittles Publishing, CRC Press, 2008:16-17,ISBN 978-1904445-30-2.
[15] EFNARC:2005 Specification and Guidelines for Self-Compacting Concrete
[16] IS 10262:2019 Indian Standard Concrete Mix Proportioning – Guidelines (Second Revision)
[17] Dennis Higgins Fifty Years of Experience in the UK using GGBS as an addition to concrete. International RILEM Conference series on Material Science – MATSCI, Aachen 2010 – Vol.III AdIPoc pg.15-20. https://www.rilem.net/images/publis/pro077-002.pdf
[18] The Trief cement process: corrosion-resisting concrete in U.K. Anti-Corrosion Methods and Materials 1955; 2:199–199. https://doi.org/10.1108/eb019071
[19] Nkinamubanzi, P.C.; Baalbaki, M.; Bickley, J.; Aitcin, P.C.The Use of Slag for Making High Performance Concrete. In Proceedings of the 6th NCB International Seminar on Cement and Bulding Materials, New Delhi, India, 24–27,1998
[20] Pal SC, Mukherjee A, Pathak SR. Investigation of hydraulic activity of ground granulated blast furnace slag in concrete. Cement and Concrete Research 2003;33:1481–6. https://doi.org/10.1016/s0008-8846(03)00062-0
[21] Provis, J.L.; Van Deventer, J.S.Alkali Activated Materials: State-of-the-Art Report; RILEM TC 224-AAM; Springer: Dordrecht, 2014:Volume 13, ISBN 978-94-007-7671-5.
[22] Provis JL, Palomo A, Shi C. Advances in understanding alkali-activated materials. Cement and Concrete Research 2015;78:110–25. https://doi.org/10.1016/j.cemconres.2015.04.013
[23] Boukendakdji O, Kadri E-H, Kenai S. Effects of granulated blast furnace slag and superplasticizer type on the fresh properties and compressive strength of self-

compacting concrete. Cement and Concrete Composites 2012;34:583–90. https://doi.org/10.1016/j.cemconcomp.2011.08.013
[24] Patra RK, Mukharjee BB. Influence of incorporation of granulated blast furnace slag as replacement of fine aggregate on properties of concrete. Journal of Cleaner Production 2017;165:468–76. https://doi.org/10.1016/j.jclepro.2017.07.125
[25] Zhang Y, Kong X. Correlations of the dispersing capability of NSF and PCE types of superplasticizer and their impacts on cement hydration with the adsorption in fresh cement pastes. Cement and Concrete Research 2015;69:1–9. https://doi.org/10.1016/j.cemconres.2014.11.009
[26] Dadsetan S, Bai J. Mechanical and microstructural properties of self-compacting concrete blended with metakaolin, ground granulated blast-furnace slag and fly ash. Construction and Building Materials 2017;146:658–67. https://doi.org/10.1016/j.conbuildmat.2017.04.158
[27] Ganesh P, Murthy AR. Tensile behaviour and durability aspects of sustainable ultra-high performance concrete incorporated with GGBS as cementitious material. Construction and Building Materials 2019;197:667–80. https://doi.org/10.1016/j.conbuildmat.2018.11.240
[28] Mehta P.K. Greening of the Concrete Industry for Sustainable Development. Concr. Int. 24, 23–28,2002.
[29] Ahmad J, Martínez-García R, Szelag M, de-Prado-Gil J, Marzouki R, Alqurashi M, et al. Effects of Steel Fibers (SF) and Ground Granulated Blast Furnace Slag (GGBS) on Recycled Aggregate Concrete. Materials 2021;14:7497. https://doi.org/10.3390/ma14247497
[30] Stöber W, Fink A, Bohn E. Controlled growth of monodisperse silica spheres in the micron size range. Journal of Colloid and Interface Science 1968;26:62–9. https://doi.org/10.1016/0021-9797(68)90272-5
[31] Garg Rishav, Garg Rajni, Bansal M, Aggarwal Y. Experimental study on strength and microstructure of mortar in presence of micro and nano-silica. Materials Today: Proceedings 2021;43:769–77. https://doi.org/10.1016/j.matpr.2020.06.167
[32] P. P. A, Nayak DK, Sangoju B, Kumar R, Kumar V. Effect of nano-silica in concrete; a review. Construction and Building Materials 2021;278:122347. https://doi.org/10.1016/j.conbuildmat.2021.122347
[33] Singh LP, Bhattacharyya SK, Kumar R, Mishra G, Sharma U, Singh G, et al. Sol-Gel processing of silica nanoparticles and their applications. Advances in Colloid and Interface Science 2014;214:17–37. https://doi.org/10.1016/j.cis.2014.10.007
[34] Wang XF, Huang YJ, Wu GY, Fang C, Li DW, Han NX, et al. Effect of nano-SiO2 on strength, shrinkage and cracking sensitivity of lightweight aggregate concrete. Construction and Building Materials 2018;175:115–25. https://doi.org/10.1016/j.conbuildmat.2018.04.113
[35] Zareei SA, Ameri F, Bahrami N, Shoaei P, Moosaei HR, Salemi N. Performance of sustainable high strength concrete with basic oxygen steel-making (BOS) slag and nano-silica. Journal of Building Engineering 2019;25:100791. https://doi.org/10.1016/j.jobe.2019.100791
[36] Qian Y, De Schutter G. Enhancing thixotropy of fresh cement pastes with nanoclay in presence of polycarboxylate ether superplasticizer (PCE). Cement and Concrete Research 2018;111:15–22. https://doi.org/10.1016/j.cemconres.2018.06.013
[37] Zahiri F, Eskandari-Naddaf H. Optimizing the compressive strength of concrete containing micro-silica, nano-silica, and polypropylene fibers using extreme vertices mixture design. Frontiers of Structural and Civil Engineering 2019;13:821–30. https://doi.org/10.1007/s11709-019-0518-6
[38] Björnström J, Martinelli A, Matic A, Börjesson L, Panas I. Accelerating effects of colloidal nano-silica for beneficial calcium–silicate–hydrate formation in cement.

Chemical Physics Letters 2004;392:242–8. https://doi.org/10.1016/j.cplett.2004.05.071
[39] Ltifi M , Guefrech A, Mounanga P, Khelidj A.Experimental study of the effect of addition of nano-silica on the behaviour of cement mortars Mounir. Procedia Engineering;2011;10:900–905. https://doi.org/10.1016/j.proeng.2011.04.148
[40] Zhang M-H, Islam J, Peethamparan S. Use of nano-silica to increase early strength and reduce setting time of concretes with high volumes of slag. Cement and Concrete Composites 2012;34:650–62. https://doi.org/10.1016/j.cemconcomp.2012.02.005
[41] Sharkawi AM, Abd-Elaty MA, Khalifa OH. Synergistic influence of micro-nano silica mixture on durability performance of cementious materials. Construction and Building Materials 2018;164:579–88. https://doi.org/10.1016/j.conbuildmat.2018.01.013
[42] Mukharjee BB, Barai SV. Influence of Incorporation of Colloidal Nano-Silica on Behaviour of Concrete. Iranian Journal of Science and Technology, Transactions of Civil Engineering 2020;44:657–68. https://doi.org/10.1007/s40996-020-00382-0
[43] Nazar i A, Riahi S.Microstructural, thermal, physical and mechanical behavior of the self-compacting concrete containing SiO2 nanoparticles. Mater Sci Eng A 2010;527:7663–72. https://doi.org/10.1016/j.msea.2010.08.095
[44] Nazar i A, Riahi S. The role of SiO2 nanoparticles and ground granulated blast furnace slag admixtures on physical, thermal and mechanical properties of self-compacting concrete. Mater Sci Eng A 2011;528:2149-2157. https://doi.org/10.1016/j.msea.2010.11.064
[45] Amin M, Abu el-hassan K. Effect of using different types of nano materials on mechanical properties of high strength concrete. Construction and Building Materials 2015;80:116–24. https://doi.org/10.1016/j.conbuildmat.2014.12.075
[46] Khaloo A, Mobini MH, Hosseini P. Influence of different types of nano-SiO2 particles on properties of high-performance concrete. Construction and Building Materials 2016;113:188–201. https://doi.org/10.1016/j.conbuildmat.2016.03.041
[47] Najigivi A, Khaloo A, Iraji zad A, Abdul Rashid S. Investigating the effects of using different types of SiO2 nanoparticles on the mechanical properties of binary blended concrete. Composites Part B: Engineering 2013;54:52–8. https://doi.org/10.1016/j.compositesb.2013.04.035
[48] Amin M, Abu el-hassan K. Effect of using different types of nano materials on mechanical properties of high strength concrete. Construction and Building Materials 2015;80:116–24. https://doi.org/10.1016/j.conbuildmat.2014.12.075
[49] IS 269:2015 Ordinary Portland Cement – Specification (Sixth revision)
[50] IS 16714-2018 Ground Granulated Blast Furnace Slag for use in cement, mortar and concrete - Specification
[51] IS 383:2016 Coarse and Fine aggregate for concrete – Specification (Third revision)
[52] IS 9103:1999 Concrete admixtures – Specification (First revision)
[53] IS 516 (Part 1/Sec 1): 2021 Hardened Concrete -Methods of Test Part 1 Testing of Strength of Hardened Concrete Section 1 Compressive, Flexural and Split Tensile Strength (First Revision)
[54] IS 456:2000 Plain and Reinforced concrete- Code of practice (fourth revision)
[55] B.D.Cullity, S.R.Stock Elements of X-ray diffraction – Third edition.2014:191-200, ISBN 13: 978-1-292-04054-7